Extended Abstracts of the 2014 International Conference on Solid State Devices and Materials, Tsukuba, 2014, pp62-63

Investigation of Low-Frequency Noise in High-k First/Metal Gate Last HfO_2 and ZrO_2 nMOSFETs

San Lein Wu[1], Bo Chin Wang[2], Yu Ying Lu[1], Shih Chang Tsai[2], Jone Fang Chen[2], Shoou Jinn Chang[2,3], Sheng Po Chang[2,3], Che Hua Hsu[4], Chih Wei Yang[4], Cheng Guo Chen[4], Osbert Cheng[4], and Po Chin Huang[2,3*]

[1] Department of Electronic Engineering, Cheng Shiu University, Kaohsiung City 833, Taiwan

[2] Institute of Microelectronics and Department of Electrical Engineering, National Cheng Kung University, Tainan City 701, Taiwan

[3] Advanced Optoelectronic Technology Center, National Cheng Kung University, Tainan City 701, Taiwan

[4] Central R&D Division, United Microelectronics Corp., Tainan City 744, Taiwan

Phone: +886-6-2757575 ext.62400-1223 Fax: +886-6-2761854 [*]e-mail: pchuang@mail.ncku.edu.tw

1. Introduction

Nowadays, CMOS technology has intruded into RF and analog circuits. Low-frequency (LF) noise, including flicker ($1/f$) noise and random telegraph signal (RTS) noise, becomes an important issue for these applications due to the excessive LF noise will lead to a limitation of in the functionality for related circuits [1], [2]. In MOSFETs, LF noise is considered stemming from the fluctuation of carriers, including trapping/detrapping behavior and/or scattering in carrier mobility [3]-[5]. On the other hand, high-k (HK) materials are adopted into advanced CMOS process for solving the increased gate leakage current and achieving low equivalent oxide thickness (EOT) [6]. However, replacing a gate insulator usually accompanies the changes of interface properties, resulting in the influence on LF noise. In this work, the LF noise characterizations of nMOSFETs with HfO_2 and ZrO_2 HK gate dielectrics are investigated by the measurements of $1/f$ and RTS noises, simultaneously.

2. Device fabrication

A 28 nm HK first/metal gate last technology was used to prepare the HfO_2 and ZrO_2 nMOSFETs. The thickness of the SiO_2 interfacial layer (IL) was approximately 1 - 1.1 nm. All HK gate stacks were deposited on the top of the SiO_2 IL by atomic-layer-deposition. The thickness of all HK gate stacks was approximately 1.6 - 1.7 nm. After the depositions of the HK layers, a TiN cap layer was deposited following the metal gate processes. The EOT is 1.248 and 1.246 nm for HfO_2 and ZrO_2 nMOSFETs, respectively. All the results of $1/f$ and RTS noises are taken from at least the average of five samples.

3. Results and Discussion

Fig. 1 show the normalize drain current noise spectral density (S_{ID}/I_D^2) versus the frequency for both devices. The S_{ID}/I_D^2 of ZrO_2 device is lower than that of HfO_2 one, implying the smaller oxide trap density (N_t) in ZrO_2 device. In addition, as compared with HfO_2 device, the "hump" shape is not so distinct in ZrO_2 device. Fig. 2 shows the frequency exponential factor of γ ($S_{VG} = S_{ID}/g_m^2 \sim f^{-\gamma}$) versus gate voltage overdrive (V_G - V_T). The γ values of ZrO_2 device are smaller than those of HfO_2 device at all $V_G - V_T$, suggesting that trap density ratio of interior trap to interface trap is smaller in ZrO_2 gate stack than that of HfO_2 one [7]. Before interpreting this differential, it has to clarify the mechanisms of $1/f$ noise first. Fig. 3 shows the S_{ID}/I_D^2 and the transconductance to drain current squared ($(g_m/I_D)^2$) as function of drain current (I_D). Different dominant $1/f$ noise mechanisms between HfO_2 and ZrO_2 devices are identified. For HfO_2 device, the S_{ID}/I_D^2 curves vary with the I_D as $(g_m/I_D)^2$, indicating the carrier number fluctuation stemming from the trapping/detrapping behaviors [8]. For ZrO_2 device, the S_{ID}/I_D^2 curves cannot follow the trend of $(g_m/I_D)^2$ at high current level, which means that either of the correlated mobility fluctuation or source/drain series resistance is possibly involved [9]. As shown in Fig. 4, the S_{ID}/I_D^2 varies V_G - V_T as $(V_G - V_T)^{-m}$ with m ~ 2 for the HfO_2 device, which confirms that noise is due to carrier number fluctuation again, and m ~ 0.99 for ZrO_2 device, which points out that the noise contribution of the series resistance can be negligible [10] and the mobility fluctuation noise is involved as an origin of the $1/f$ noise. In other words, the dominant $1/f$ noise mechanism in ZrO_2 device is the correlated number-mobility fluctuation, i.e., unified model [11].

The Hooge's parameter ($\alpha_H = fWLC_{OX}|V_G - V_T|S_{ID}/qI_D^2$) is also considered as a figure of merit for both devices [12]. The calculated α_H values are illustrated in Fig. 5 as a function of V_G - V_T. As expected, the lower α_H in ZrO_2 device are observed. For HfO_2 device, it can be seen that the reduction in α_H as $V_G - V_T$ increased. This is because increased $V_G - V_T$ induces more free carriers in channel, and then the trapping/detrapping behaviors from HK film are screened and become unobvious. On the other hand, Fig. 6 shows the calculated carrier number in channel and $1/4\pi\alpha_H$ versus V_G - V_T. For both devices, the carrier number at all $V_G - V_T$ is smaller than the $1/4\pi\alpha_H$, indicating the occurring possibility of RTS noise.

A distinct difference in I_D between two states is observed as shown in Figs. 7 and 8 for HfO_2 and ZrO_2 device, respectively, which confirms that the RTS noise exists in both devices. The extracted mean capture time (τ_c) and the mean emission time constant (τ_e) versus V_G - V_T are presented in Fig. 9. The trap positions in insulator, including vertical location (X_T) and lateral location (Y_T), can be extracted from the data of Fig. 9 [13]. The X_T is 1.81 and 0.44 nm, and the Y_T is 16.40 and 24.44 nm for HfO_2 and ZrO_2 device, respectively. These results of RTS noise mean that the electron trapping behavior in HfO_2 device is more serious. In addition, the RTS noise contributes a Lorentzian shaped S_{ID}/I_D^2 in LF spectrum. Therefore, the obvious "hump" shaped S_{ID}/I_D^2 of HfO_2 in Fig. 1 can be reasonably explained by the stronger contribution of RTS noise.

The relation between the X_T and the tunneling attenuation length for channel carriers penetrating into the gate dielectric (λ) is revealed according to an equation as $X_T = \lambda \ln(1/2\pi f \tau_0)$ [14]. The λ values are calculated as 1.01×10^{-8} and 0.24×10^{-8} cm for HfO_2 and ZrO_2 device, respectively. The N_t value can be further obtained from the measured $1/f$ noise results using the following formula [15]:

$$\frac{S_{ID}}{I_D^2} = \frac{\lambda kT}{fWL}\left(\frac{1}{N} + \frac{\mu}{\mu_{C0}\sqrt{N}}\right)^2 N_t \qquad (1)$$

where N is the carrier density of the inversion layer, and μ is the field effective mobility. The extracted N_t versus V_G - V_T is illustrated in Fig. 10. The N_t values of ZrO_2 device are lower than those of HfO_2 device. The interface trap (N_{it}) is also extracted by charge pumping measurement as shown in Fig. 11. It can be seen that the increase of N_{it} in HfO_2 device is rapider than that of ZrO_2 counterpart as the pulse period raised. It suggests the defects in internal HfO_2 gate stack is higher as compared with ZrO_2 gate stack, which agrees with our results of LF noise. The distinguishable interface properties between HfO_2 and ZrO_2 devices can be explained by the number and spatial distribution of defects in energy band diagram of the HK film. As compared to ZrO_2, the number of oxygen vacancy, which can play a role as the electron trapping site, is higher in HfO_2 and the electron traps are located in shallower levels near conduction band [16]. Therefore, electron can tunnel over the ultra-thin IL and then be trapped in HfO_2 HK films. Consequently, the serious degradation in interface properties and LF noise in HfO_2 device is observed.

4. Conclusions

In this study, we have systematically investigated the LF noise behaviors in HK first/metal gate last HfO_2 and ZrO_2 nMOSFETs by $1/f$ and RTS noise. As compared with HfO_2 film, the electron trapping behavior from ZrO_2 film is not so severer. As a result, the LF noise characterizations are improved in ZrO_2 nMOSFETs. Besides, the mechanism of LF noise is described by the carrier number fluctuation and the unified model for HfO_2 and ZrO_2 nMOSFETs, respectively.

Acknowledgements

The authors would like to thank the Advanced Optoelectronic Technology Center of NCKU for the financial support under Contract HUA103-3-15-178, the National Science Council of Taiwan for the financial support under Contract numbers NSC102-2221-E-230-015 and NSC102-2221-E-006-259, and UMC staffs for their helpful supports.

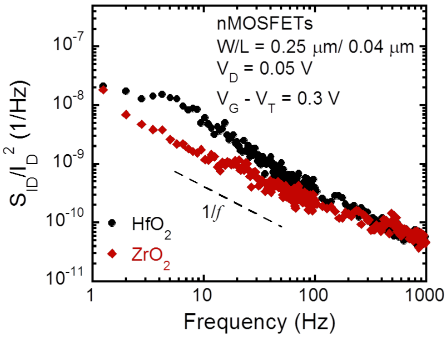

Fig. 1 Normalized drain current noise spectral density (S_{ID}/I_D^2) versus the frequency of HfO_2 and ZrO_2 nMOSFETs.

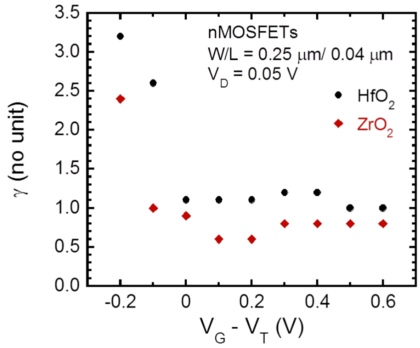

Fig. 2 Extracted frequency exponential factor of γ (S_{VG} ~$f^{-\gamma}$) versus gate voltage overdrive (V_G - V_T) of HfO_2 and ZrO_2 nMOSFETs from the results of 1/*f* noise measurement.

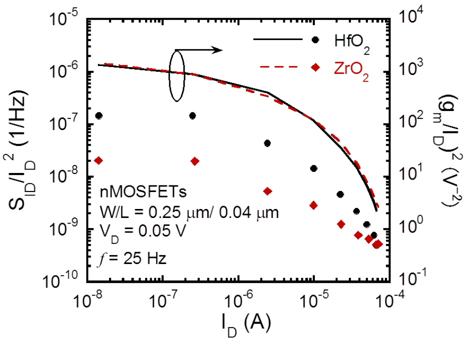

Fig. 3 Normalized drain current noise spectral density (S_{ID}/I_D^2) and transconductance to drain current ratio squared ($(g_m/I_D)^2$) versus drain current (I_D) of HfO_2 and ZrO_2 nMOSFETs.

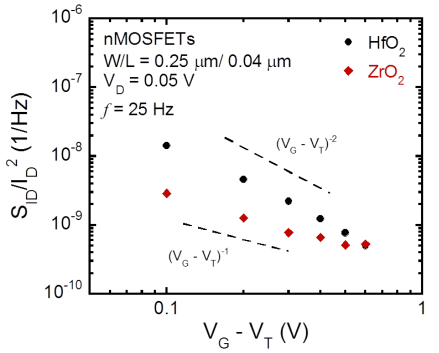

Fig. 4 The normalized drain current noise spectral density (S_{ID}/I_D^2) versus gate voltage overdrive (V_G - V_T) of HfO_2 and ZrO_2 nMOSFETs.

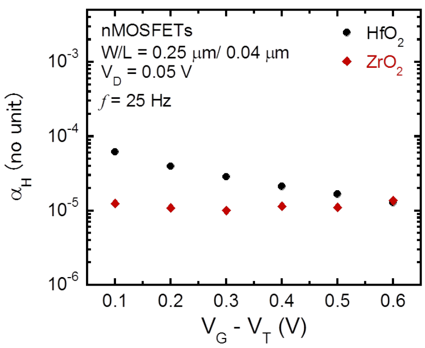

Fig. 5 Hooge parameter (α_H) versus gate voltage overdrive (V_G - V_T) of HfO_2 and ZrO_2 nMOSFETs.

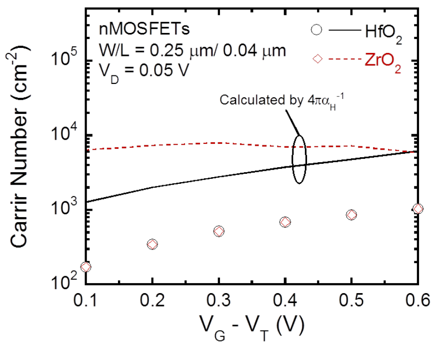

Fig. 6 Carrier number in channel and calculated $1/4\pi\alpha_H$ versus gate voltage overdrive (V_G - V_T) of HfO_2 and ZrO_2 nMOSFETs.

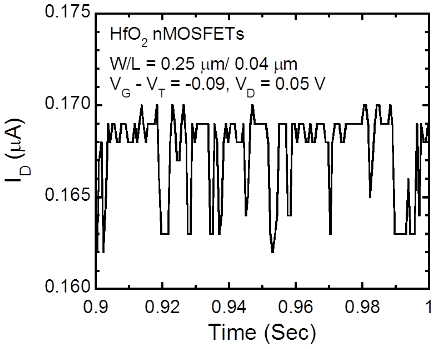

Fig. 7 Typical drain current (I_D) fluctuations of HfO_2 nMOSFETs devices in RTN measurements.

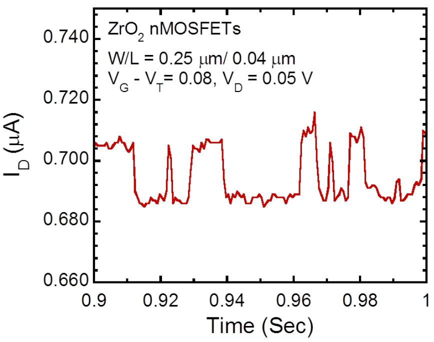

Fig. 8 Typical drain current (I_D) fluctuations of ZrO_2 nMOSFETs devices in RTN measurements.

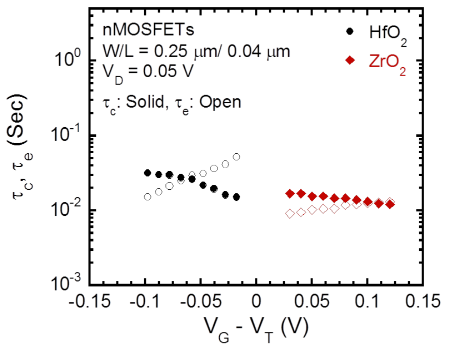

Fig. 9 The mean capture time (τ_c) and emission time (τ_e) versus gate voltage overdrive (V_G - V_T) of HfO_2 and ZrO_2 nMOSFETs.

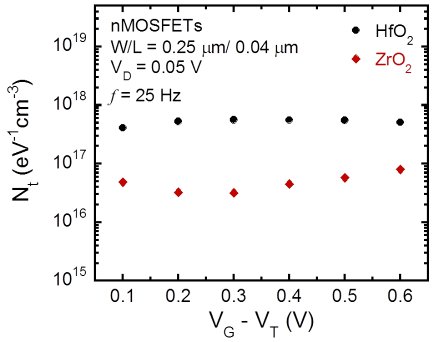

Fig. 10 Extracted oxide traps (N_t) versus gate voltage overdrive (V_G - V_T) of HfO_2 and ZrO_2 nMOSFETs from the results of 1/*f* noise and RTN measurements.

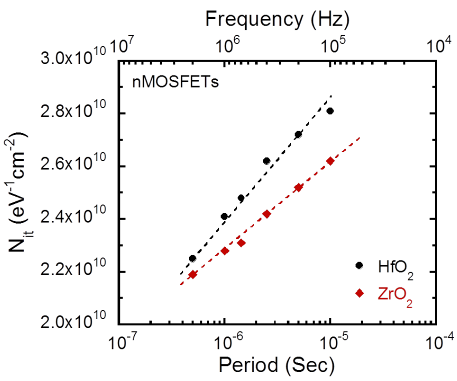

Fig. 11 Extracted interface traps (N_{it}) versus gate pulse period/frequency of HfO_2 and ZrO_2 nMOSFETs from the results of charge pumping measurement.

Reference

[1] Y. Nemirovsky *et al.*, *IEEE TED*, 921 (2001) [2] Y. Yasuda *et al.*, *IEDM*, 1 (2006) [3] K. K. Hung *et al.*, *IEEE TED*, 654 (1990) [4] G. Ghibaudo and T. Boutchacha, *Microelectron. Reliab.*, 573 (2002) [5] S. C. Tsai *et al.*, *IEEE EDL*, 834 (2013) [6] H.-S. Jung *et al.*, *Symp. VLSI Tech. Dig.*, 232 (2005) [7] M. Sato *et al.*, *Symp. VLSI Tech. Dig.*, 66 (2008) [8] H Y Lin *et al.*, *Semicond. Sci. Technol.*, 105022 (2008) [9] P. C. Huang *et al.*, *IEEE TED*, 1635 (2011) [10] L. K. J. Vandamme, *IEEE TED*, 2176 (1994) [11] F. Crupi *et al.*, *IEEE EDL*, 688 (2006) [12] L. K. J. Vandamme and F. N. Hooge, *IEEE TED*, 8 (2008) [13] B. C. Wang *et al.*, *JJAP*, 02BC11 (2012) [14] S. C. Tsai *et al.*, *J. Nanomaterials*, 787132 (2014) [15] E. P. Vandamme *et. al.*, *IEEE TED*, 2146 (2000) [16] J. Robertson, *Rep. Prog. Phys.*, 327 (2006).